Localization of surface acoustic waves in a one-dimensional quasicrystal

L. Macon,* J. P. Desideri, and D. Sornette
Laboratoire de Physique de la Matière Condensée, Université de Nice–Sophia Antipolis, Parc Valrose, 06034 Nice CEDEX, France
(Received 15 January 1991)

We present and interpret experimental results on the propagation of surface acoustic waves on a quasiperiodically corrugated solid. The surface is made of a thousand grooves engraved according to a Fibonacci sequence. This type of one-dimensional system has been much studied theoretically in the literature in the context of electronic or phonon propagation. It exhibits many interesting transport features that recall some properties of strongly disordered systems related to Anderson localization. We report precise results on the reflection and transmission frequency dependence as well as on the temporal impulse response of the system. The experimental results recover nicely the features that have been predicted. In particular, this type of system has been conjectured to correspond to a critical regime of the localization transition. By comparing two systems of different lengths, we indeed observe a characteristic signature of the criticality, related to the asymptotic approximation of the quasicrystal by periodic subsystems of increasing periods. This case is intermediate between a regime of extended proper modes associated with a continuous spectrum and a regime of localized modes corresponding to a pure-point spectrum.

I. INTRODUCTION

Wave propagation in one-dimensional ($d=1$) systems has been the focus of intense research[1–7] and is still the subject of interesting developments especially when one considers this problem in unfamiliar contexts,[1,2] which can raise additional experimental and theoretical questions. It is well known that wave propagation in disordered structures leads to the phenomenon of Anderson localization[8] at any nonvanishing disorder for $d=1$. In $d=2$, the general belief gives a conclusion similar to the ($d=1$) case, whereas a localization transition is predicted in $d=3$ (Refs. 1 and 9) and separates an extended regime at "small" disorder from a "localized" regime at "large" disorder. The localization regime is a subtle nonperturbative effect involving coherent interference between all the wavelets partially reflected by the quenched disordered set of scatterers. The existence of a localization transition, for $d=3$ and above, is particularly interesting and its study remains an important challenge of theoretical and experimental physics. Many questions are still partly or completely unresolved such as the discovery of a clear physical scenario for it, the nature of the transition, its upper critical dimension above which mean-field behavior appears, etc.). The existence of a transition between two regimes is very exciting because one can always hope that understanding the crucial features that trigger the transition will allow one to unravel the physics of the different regimes.

In this respect, ($d=1$) systems appear to be, at first sight, not as interesting as ($d=3$) systems due to the absence of a transition (the extended regime does not appear except at zero disorder). Also, for $d=1$, no "topological" disorder exists, a fact that allows one to number the scatterers sequentially and leads to very efficient transfer matrix approaches,[10] which have no real counterpart in $d=3$. Problems of ($d=1$) propagation are thus poor models for their ($d=3$) counterparts. However, they constitute the best known systems both at the theoretical[1] and experimental[11–15] level due to the relative ease of their study and the strength of the experimental effects compared to the two- or three-dimensional case.[16–22]

Following the experimental discovery by Shechtman *et al.*[23] of a metallic solid phase of Al-Mn alloy with icosahedral symmetry (i.e., a point symmetry which is inconsistent with conventional lattice translations and characterizes what are now called quasicrystals), the above classification has evolved. This is due to the fact that additional propagation behaviors have been described in one-dimensional quasiperiodic systems.[24,25] Indeed, it has been discovered that wave propagation in ($d=1$) quasiperiodic systems could also present a transition from an extended to a localized regime as it is predicted in ($d=3$) disordered systems.[1] From our point of view, this property revives considerably the interest in wave propagation in one-dimensional systems.

In this paper we present experimental results and their interpretation on the propagation of surface acoustic waves on a quasiperiodically corrugated solid. A short account of this work has already been published in Ref. 2. In the systems that are considered here, the surface of a piezoelectric substrate is corrugated by a thousand grooves engraved according to a Fibonacci sequence. Each groove acts as a single scatterer. This type of one-dimensional Fibonacci sequence has also been much studied theoretically in the literature in the context of electronic or phonon propagation. It exhibits many interesting transport features which recall some properties of strongly disordered systems related to Anderson localiza-

tion. We report precise results on the reflection and transmission frequency dependence and on the temporal impulse response of the system. The experimental results which have been obtained address theoretical results predicted in other systems. In particular, this type of systems has been conjectured to correspond to a critical regime of the localization transition, characterized by a specific critical scaling of the spectrum and by critical proper modes which are neither extended nor localized. We observe a characteristic signature of this criticality related to the asymptotic approximation of the quasicrystal by periodic subsystems of increasing periods. This case is intermediate between a regime of extended proper modes associated with a continuous spectrum and a regime of localized modes corresponding to a pure-point spectrum. We have also studied the Fourier transform of the corrugated surface by optical diffraction in absence of acoustics in order to test the spatial structure as would be done in a real quasicrystal probed by scattering techniques.

From a general point of view, the problem of wave propagation in quasiperiodic systems is interesting for several reasons:

(a) It is a natural intermediate case between periodicity and randomness. In a quasiperiodic system, two or more incommensurate periods are superimposed,[26] so it is neither a periodic nor a random system and can indeed be considered as intermediate between them.

(b) This statement is reinforced, as already mentioned, by the discovery[24] that wave propagation in $(d=1)$ quasiperiodic systems could also present a transition from an extended to a localized regime as it is predicted in $(d=3)$ disordered systems.[1]

(c) Following the recent experimental discovery of the quasicrystal phase in metallic alloys,[18] there has been a renewal of interest in the studies of the physical properties of quasiperiodic systems in one dimension referring back to earlier works.[27]

(d) This problem is also related to electron properties of incommensurate linear structures[28,29] [such as those of $K_2Pt(CN)_4 \cdot 3H_2O$, of tetrathiafulvalene-tetracyanoquinodimethane, of mercury chains in $Hg_{3-\delta}AsF_6$, (Ref. 30)] and to the fine structure of the de Haas–van Alphen[27] and other quantum oscillations in high magnetic fields.

(e) From a different point of view, studying the interaction of elastic surface acoustic waves with complex surface topography[31,32] is of major importance to underwater acoustics, seismology, surface acoustic wave devices, nondestructive testing, and ultrasonic applications in medicine. Quasiperiodic structures could also provide useful systems for analogical coding, multiband filters, discretization, and integrated analogical frequency analyzer.

A lot of theoretical works[33–53] have been concerned with the localization properties of quasiperiodic $(d=1)$ lattices essentially focusing on the tight-binding discrete Schrödinger equation

$$t_{n+1}Y_{n+1}+t_{n-1}Y_{n-1}+(V_n-E)Y_n=0 ,$$

where the coefficients $t_{n\pm1}$ represent the "hopping" term at sites $n\pm1$ and E is the eigenenergy. V_n is the local value of the potential at site n. The most important models which have been studied theoretically in the literature are the following.

(i) In the Aubry model, the scatterers are equidistant but have *scattering cross sections* quasiperiodically modulated: $t_{n-1}=t_{n+1}=T$ is constant and $V_n=V\cos(2\pi n\sigma)$, where σ is an irrational number. For $V>2T$, all eigenfunctions are localized and the spectrum is pure point whereas for $V<2T$, all eigenfunctions are extended and the spectrum is continuous. The case $V=2T$ corresponds to the critical localization transition.

(ii) An alternative model consists of identical scatterers whose *positions* are quasiperiodically modulated. A much studied case is given by $x_n=A\cos(2\pi n\sigma)$ and $V_n=V$ is a constant. Note that for σ irrational, x_n covers densely and uniformly the interval (i.e., is ergodic). In contrast to the previous case, there is no energy-independent transition from all extended to all localized eigenfunctions as the strength of the modulation is increased since the ratio of E/T is no longer constant but depends continuously on the wave frequency.

(iii) As in (ii), the scatterers are identical ($V_n=V$) but with *separations* which takes only two values "*s*" and "*c*" which occur according to formula (1) (see below) building a self-similar so-called Fibonacci structure with remarkable properties. This model is believed to be quite similar to the Aubry model for the particular value $V=2T$ corresponding to the critical localization transition.

(iv) Other systems with various approaches and some experiments have been recently tackled which we just mention for completeness.[3–7]

On the experimental side,[54–57] a few works have been reported on semiconductor superlattices, which have mainly focused on the study of their structural, dynamical, electronic, and optical properties in relation to the quasiperiodicity. The analogous problem of acoustical or optical wave propagation in quasiperiodic lattices has been much less studied theoretically[47,50] and there are relatively few experimental results in this field.[58] Actually, experimental results exist in $(d=1)$ for classical waves, such as acoustic, electromagnetic, mechanical, or hydrodynamical waves, but only for periodic and random systems. Indeed, localization has already been observed for surface waves in hydrodynamics,[11] in acoustics for the transverse vibration of a rope,[12,14] or for the propagation in tubes notched with random holes,[13] for third or fourth sounds in helium fluid.[15] Related works on other physical systems can also be found in Refs. 25 and 59–61.

In Ref. 62, Smith *et al.* have reported interesting experimental results on the propagation of third sound in superfluid helium propagating above a corrugated quasiperiodic system of abraded strips. Their system contained about 100 scatterers, with each possessing a relatively high reflecting efficiency. This third-sound experiment was found to be quite convenient for several reasons: (1) at sufficiently low temperatures, the intrinsic attenuation length for waves propagating on uniform substrates can be made extremely large. (2) The interaction between excitations (i.e., the existence of nonlinear coupling) can be made arbitrarily small by controlling

their amplitude. (3) The scatterers are macroscopic and can be built essentially identical to each other. (4) The scattering efficiency of each scatterer is relatively high so that clear signatures of Anderson localization can be observed.

Our systems share the advantages of presenting a small intrinsic dissipation, a controllable nonlinearity, and an extremely well-controlled scatterer geometrical structure. Each scatterer used in our systems possesses a rather small reflecting efficiency (of order 1% in amplitude per scatterer). However, we have used much longer systems (containing 1000 and 2000 grooves). The main interest of using long systems stems from the possibility of exploring the rich scaling structure of the "spectrum" (i.e., the dependence of the transmission and reflection coefficients on frequency) and the internal spatial structure of the surface-acoustic-wave proper modes. Note, furthermore, that our systems can be analyzed with a very high precision (better than 10^{-5} in relative frequency position), thus enabling the detection of very fine details in the system spectrum.

Zhu *et al.*[25] have studied experimentally and numerically the band structure of mechanoelectric transducers made of a Fibonacci system of elementary surface acoustic sources. The band structure of these transducers is simply obtained by spatial Fourier transform of the spatial Fibonacci sequence describing the position of the acoustic sources. Their results[25] are thus very similar to those presented in Sec. III B concerning the Fourier transform by optical diffraction of the quasicrystal.

The structure of the paper is the following. In Sec. II we present the experimental acoustic set-up. In Sec. III we discuss the experimental results and their interpretation for the system of grooves engraved according to a Fibonacci sequence. We first introduce the system which is studied (Sec. III A), describe its Fourier transform obtained by an optical diffraction experiment (Sec. III B), study the acoustic spectrum both experimentally and numerically (Sec. III C), and finally present the acoustic time impulse response of the system (Sec. III D). In the discussion of our experimental results, we adapt known theoretical approaches to the specificity of our problem in conjunction with numerical calculation. Section IV contains our conclusions and we discuss some open problems. Appendix A presents the analogy between the SAW propagation on a corrugated surface and the tight-binding discrete Schrödinger model for electronic transport in a random or quasiperiodic potential. Appendix B summarizes and adapts the approach of Kohmoto *et al.*[33,36,38,39] to our system; it amounts to relating the transfer matrix formalism presented in Appendix A to dynamical mapping theory.

II. DESCRIPTION OF THE EXPERIMENTAL SET-UP AND OF ITS CHARACTERISTICS

We have studied a lattice of identical grooves engraved at the surface of a piezoelectric lithium niobate $LiNbO_3$ substrate, using well-known microlithographic techniques.[31] A schematic representation of the experimental system is represented on Fig. 1(a). Figure 1(b) presents

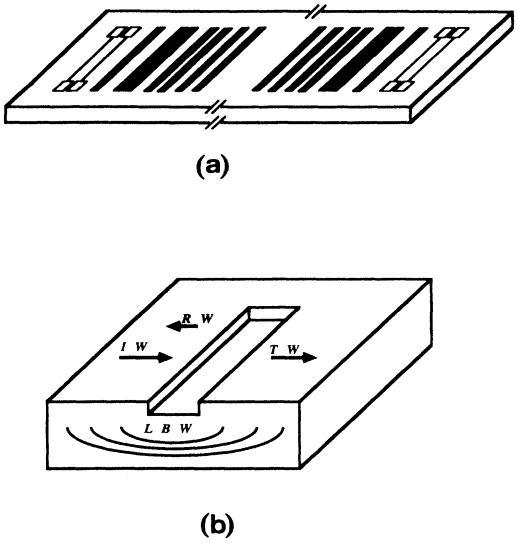

FIG. 1. (a) Schematic representation of the experimental system. Each pair of "dumbbells" on both sides of the lattice of grooves depicts a SAW transducer working either in reflection or in transmission. The propagating path is perpendicular to the array of grooves, along the large axis of the system. (b) Detail of a groove. *IW* stands for incident wave, *RW* for reflected wave, *TW* for transmitted wave, and LBW for a leaky bulk wave.

the geometry of a single groove of width $w=5$ μm, depth $h=0.3$ μm, and identical-well-characterized profile resembling an inverse plateau. The lateral scale of each groove (the so-called opening) is $E=2150$ μm. We have verified, by probing the SAW intensity profile in the direction transverse to the system of grooves axis using the optical diffraction technique described below, that the SAW propagation was correctly directed along the lattice axis, thus preventing the existence of any "beam walk-off."

The array of grooves is surrounded by electromechanical transducers, laid down onto the surface of the $LiNbO_3$ crystal, performing transmission and reception of the surface acoustic waves. A transducer is generally a periodic structure of alternate electrodes (so-called interdigital structure) connected to two buses, themselves connected to the terminals of either an electric generator or an analyzer. The spectral response of the quadrupole constituted by the two transducers is centered around a frequency corresponding to the periodicity of the fingers of the transducers, with a 3-dB bandwidth depending upon the number of pairs of interdigital electrodes (typically, the frequency f is in the range 10 MHz to 2 GHz and the relative bandwidth is $\Delta f/f \sim 20\%$ for an interdigital electrode structure of three periods). These characteristics can be somewhat adjusted by an appropriate electrical surrounding.

In practice we must allow for a number of secondary effects, among which predominate mutual reflections between transducers and between the later and the array, reflections from the edges of the crystal, transmission of

bulk waves by the transducers and the grooves which can be reinjected at the surface after reflection from the bottom of the crystal, electromagnetic radiated noise from the excited transducers. These different perturbative effects have been recognized[31] for a long time and can be either minimized by a suitable optimization of the structure or separated from the interesting information in the signal treatment. We will address these points, when necessary, during the exposition of the corresponding experimental results.

The surface acoustic wave (SAW) which has been studied is the Rayleigh wave whose characteristics for a perfect solid surface in contact with void are well known.[63] Rayleigh SAW constitutes a particular type of elastic wave in solids and can be seen as a mixture of longitudinal and transverse waves such that the condition of vanishing stress at the free solid boundary is fulfilled. They are characterized by a real wave vector in the directions parallel to the surface and a pure imaginary wave-vector component in the direction perpendicular to the surface. The SAW thus propagates along the plane and is evanescent away from the solid boundary with a typical excursion of the order of the wavelength. Rayleigh SAW propagate with a phase velocity c_R slightly less than the phase velocity c_t of the transverse (or shear) bulk wave. The dispersion relation of the Rayleigh SAW is linear ($\omega = c_R k$) in absence of corrugation. In the presence of a perturbation to the planar shape (take, for example, the case of the existence of a single groove of depth h and width w), the SAW is partially reflected with a reflection amplitude coefficient given by $\mu \approx 0.6(h/\lambda)\sin(2\pi w/\lambda)$ (Refs. 55–61) ($\approx 4\times 10^{-3}$ for our frequency range $f \approx 160$ MHz). Furthermore, a fraction $p \sim 20\mu^2$ of the SAW energy is detrapped and converted into longitudinal and shear bulk acoustic waves.[64–70] Note also that the consequence of the presence of air instead of void has been well documented and is known to lead to a small well-controlled additional loss.[31]

In the general context of wave propagation in inhomogeneous systems, SAW are particularly interesting for several reasons which we have exploited in our experiments.

Rayleigh waves are well defined in frequency (for instance, with a precision of 1 kHz around a main frequency of 100 MHz corresponding to a relative precision of 10^{-5}). The intensity of the wave can also be precisely monitored and kept far away from nonlinear thresholds. The wave fronts can be made planar to a good accuracy and controlled by different techniques.[31]

All the characteristics of the propagation phenomena (spectra, time response, modal structures) can be extracted experimentally. This feature is particularly interesting for testing predictions of theoretical models.

SAW propagation suffers from a relatively weak intrinsic dissipation (without speaking of the attenuation due to the leakage of the guided SAW from the corrugated surface into the bulk which is discussed below).

The solid which we have used is a piezoelectric lithium niobate substrate (PLNS). Rayleigh SAW propagating at the surface of PLNS are often used to develop devices with many industrial applications. For example, real-time signal processing in radar or in television sets use Rayleigh acoustic waves propagating at the surface of a piezoelectric solid.[31] In particular, surface acoustic waves, propagating on reflective arrays constituted of parallel grooves, have numerous applications (reflective array compressors, bandpass filters, filters banks, high performance SAW resonators, oscillators).[31] We have therefore benefited from the well-developed and efficient available technology for preparing well-controlled corrugated surfaces.

Our experimental results are obtained as follows. We sample the frequency range of interest with a typical frequency step of 3 kHz. The temperature of the sample is regulated at ± 1 %C and the spectral response of the quadrupole is measured with a precision better than 10^{-2} dB. Because of the limited 3-dB bandwidth of the transducers, which is in the range of 30 MHz around 160 MHz, the time impulse width is not vanishing but around 0.03 μs. This allows us to distinguish SAW paths with length difference of the order or larger than 100 μm.

III. STUDY OF THE ($d = 1$) QUASICRYSTAL

A. Structural characteristics

The system, which has been studied is constituted of a lattice of $N = 1000$ grooves of identical width $w = 5$ μm, depth $h = 0.3$ μm, and an identical well-characterized profile resembling an inverse plateau [Fig. 1(b)]. The total length of the 1000 grooves system is $L = 15\,984$ μm giving an average groove spacing $a = 15\,984/999 = 16$ μm. The first groove is placed at a position which is taken as the origin. Then, a specific deterministic method is used to generate the successive spacings between neighboring grooves. A simple representation of the projection method used to construct these spacings between grooves is presented on Fig. 2. It illustrates in the one-dimensional case an elegant and general way of generating a wide class of almost periodic tiling of Euclidean d-dimensional space by projection from higher-dimensional regular lattices, in direct (position) space.

Consider in the Euclidean plane R^2, the strip swept by shifting the unit square ($-1 < x \leq 0$; $0 < y \leq 1$) along the straight line D of the equation $y = \sigma x$ where $\sigma = \tan\theta$ and θ is the angle between D and the x axis. By projecting orthogonally onto D all points of the strip having integer coordinates, we get a sequence of points on D (see Fig. 2) which build the announced quasicrystal. Let us note x_n the abscissa along D of the point number n, assuming that the label $n = 0$ is attached to the origin. The distance $l_n = x_{n+1} - x_n$ of the bond joining point n and $n+1$ (and thus the distance between neighboring grooves in our system) can only take two values $s = \sin\theta$ and $c = \cos\theta$, corresponding, respectively, to the projections of vertical or horizontal segments of the original lattice Z^2.

In the following we shall treat in detail the case where the irrational number σ is the inverse golden mean $t = (t+1)^{-1} = (5^{1/2}-1)/2 = 0.6180$ keeping in mind that the specific results obtained for this particular value are

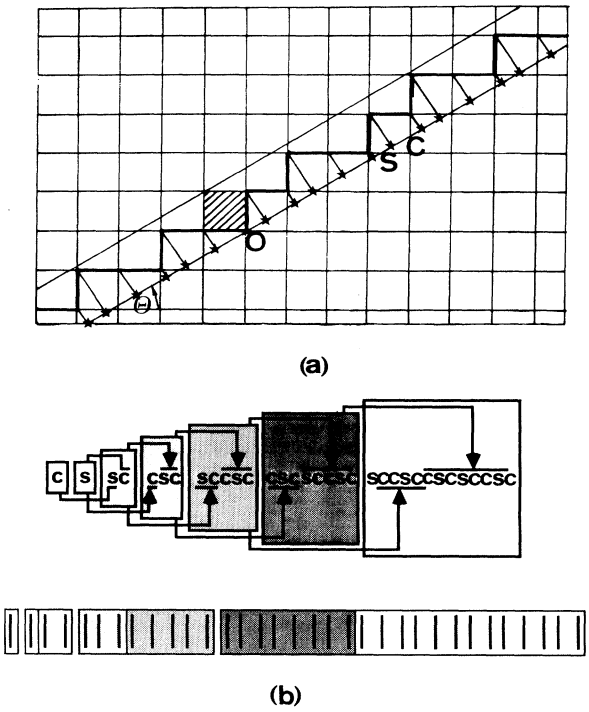

FIG. 2. (a) Simple representation of the projection method used to construct the Fibonacci spacings between grooves. (b) Geometrical illustration of the concatenation procedure given in Eq. (1), which constitutes another alternative method to construct the Fibonacci sequence.

generalizable to values of σ which have the most typical diophantine properties, i.e., are not too well approximated by rationals. The inverse golden mean is special in the sense that it contains only the number 1 in its continued fraction expansion

$$\cfrac{1}{r_1+\cfrac{1}{r_2+\ddots+\cfrac{1}{r_n+\cfrac{1}{x}}}}$$

i.e., $r_1=r_2=r_3\cdots=r_n=\cdots=1$. Hence, it is the irrational number that is the worst approximated by rationals, and thus the number for which the lack of periodicity of our quasicrystal is expected to have quantitatively the most spectacular consequences.

Complementary to the geometric construction presented in Fig. 2, the sequence of spacing can be obtained from a simple recursion relation on the sequence of "letters" s $(=\sin\theta)$ and c $(=\cos\theta)$ corresponding to the succession of groove distances along the system. Denoting S_j the sequence of s and c at the jth iteration, one has[26,35]

$$S_{j+1}=\{S_{j-1}S_j\} \quad \text{for } j \text{ odd}$$
$$=\{S_jS_{j-1}\} \quad \text{for } j \text{ even}, \qquad (1)$$

where multiplication is to be understood as word concatenation. This construction is depicted in Fig. 2(b). The initial values of the recursion are $S_0=s$ and $S_1=c$, where s and c are two chosen distances which constitute the two elementary tiles used for creating the quasicrystal. Since a finite number of elementary tiles (here two) are used to build the system quasiperiodically, the structure can be termed a quasicrystal.[23,71] With the recursion (1), one has $S_2=\{sc\}$, $S_3=\{scc\}$, $S_4=\{scscc\}$, and so forth. It is easy to verify that the nth letter $W(n)$ (which is either "s" or "c") of the word S_j is given by the formula

$$W(n)=s-(c-s)\mathrm{Int}\{\mathrm{Frac}[(n-1)(1-t)]-t\}$$
$$\text{for } n\geq 2 \qquad (2)$$

which is another way of reconstructing explicitly the sequence (1) with $W(1)=s$. In Eq. (2), the function $\mathrm{Int}(x)$ $[\mathrm{Frac}(x)]$ means the integer (fractional) part of x. They verify $\mathrm{Int}(-x)=-[1+\mathrm{Int}(x)]$ for ($x>0$ and x noninteger) and $\mathrm{Int}(-x)=-\mathrm{Int}(x)$ for ($x>0$ and x integer). Also, $\mathrm{Frac}(x)=1+\mathrm{Int}(x)-x$ for ($x>0$ and x noninteger) and $\mathrm{Frac}(-x)=0$ for ($x>0$ and x integer). This implies that the usual definition $\mathrm{Int}(x)+\mathrm{Frac}(x)=x$ is verified for all x positive or negative. From Eq. (2) one verifies that $W(2)=c$, $W(3)=s$, $W(4)=c$, $W(5)=c$, and so on. Variants of the concatenation described by Eqs. (1) and (2) can be used[2] which do not change the properties described below.

In a system S_j built from the above recurrence up to j, there are F_j grooves where F_j is a Fibonacci number given recursively as $F_{j+1}=F_j+F_{j-1}$ with $F_0=F_1=1$.[72] In our experimental system we have chosen $s=22\sin\theta$ $\mu m\approx 11.6\pm 0.1$ μm and $c=22\cos\theta$ $\mu m\approx 18.7\pm 0.1$ μm, where $\tan\theta=t$, as the values of the two distances between the groove centers found in the Fibonacci sequence, yielding $s/c=0.620\pm 0.005$ near the inverse golden mean $t=(\sqrt{5}-1)/2=0.6180$. The ± 0.05 μm precision of the position of the grooves corresponds to the limitation of the electronic etching method used for preparing the system. The average distance between the grooves [see Eq. (10) below for a definition] is a $L/999=16$ μm.

B. Fourier transform by optical diffraction of the ($d=1$) quasicrystal

Before studying the acoustical transport properties of these systems, we report on an experiment giving the direct spatial Fourier transform of the whole set of grooves. This is useful in order to probe the quality of the preparation of the quasicrystalline structure with an independent method. Secondly, the spatial Fourier spectrum is interesting in its own right since it is the one-dimensional counterpart of the experimental spectrum obtained from scattering techniques on real metallic alloys $d=3$ quasicrystals.[71]

The diffraction pattern of a quasicrystal is one of its more distinctive features. Quasiperiodic systems possess the remarkable property that their diffraction patterns are made of a dense series of Bragg peaks, although being absolutely not periodic. Bragg diffraction peaks have

been long thought to be the only associated to scattering of waves by purely periodic systems. The surprising discovery of quasiperiodic crystals have shown that this is indeed not true and that a larger class of systems, without periodicity, do exhibit Bragg peaks. The experiment which is reported below illustrates this fact.

In Fig. 3 we present the optical diffraction pattern of a quasicrystalline system of 2280 grooves partitioned following the Fibonacci sequence (1). Care has been taken to illuminate the whole sample as uniformly as possible. Note that due to the finite size of the system, the Bragg peaks are broadened.

The optical diffraction is the Fourier transform $\Phi(k)$ of the lattice and exhibits self-similar properties reminiscent of those of the lattice (on the quasicrystal lattice, one can eliminate a subset of the lattice grooves and obtain another quasiperiodic lattice with nearest-neighbor distances increased by a constant factor). $\Phi(k)$ is the product of the Fourier transform $F(k)$ of the lattice of points centered on each grooves by the Fourier transform $f(k)$ of the single-groove form function, with

$$F(k)=\text{Fourier transform of}\sum_n \delta(x-x_n)\ , \tag{3}$$

where the points x_n belong to the Fibonacci sequence. Several methods exist for computing $F(k)$ based on projection from a higher dimensional periodic lattice, on a density wave description of icosahedral quasicrystals, on the generalized dual method, or on multigrid methods.[73] From Ref. 71 one has

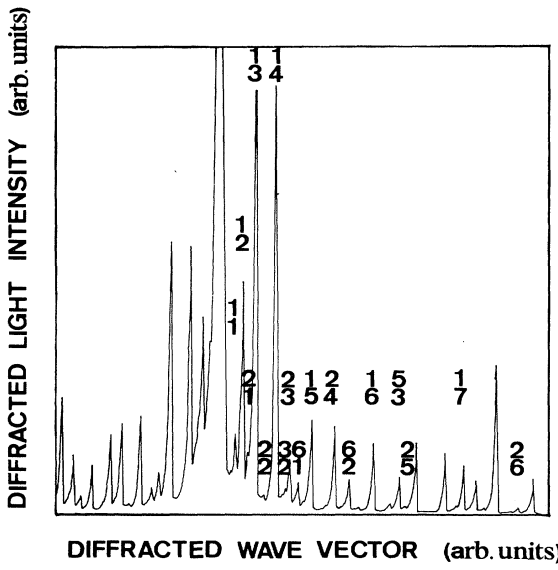

FIG. 3. Optical diffraction pattern of the quasicrystalline system of 2280 grooves partitioned following the Fibonacci sequence. Several families of peaks are indicated which occur in geometrical progression (for each order of diffraction). The expression of the wave vector corresponding to the strongest peaks is given by Eq. (8). This striking prediction is very clearly verified on the figure. It is possible to identify the families of peaks ($l=1, n=1-7$), ($l=2, n=1-6$), etc.

$$F(k)=\sum_{p,q}\{\sin(X/2)/(X/2)\}e^{i\gamma}\delta(k-k_{pq}) \tag{4}$$

with

$$k_{pq}=(2\pi/a)(pt^{-1}+q)\ , \tag{5}$$

$$X=(2\pi/\sqrt{5})(qt^{-1}-p),\quad \gamma=X/2\ , \tag{6}$$

where a is again the average distance between the grooves. p and q are two integers. Expression (4) and (5) shows that the Fourier transform of the lattice consists in a dense set (of zero measure since this is the set of rationals) of Bragg peaks indexed by (p,q). Experimentally, only the brightest peaks will be seen. They correspond to the maxima of $F(k)$ as given by Eq. (4) which occur when $X\approx 0$. The smallest values of X are reached for special values of p and q which are the best approximates of the golden mean. These best approximates are, by definition, the Fibonacci numbers $p=F_n$ and $q=F_{n-1}$ such that p/q gives the best approximation to t^{-1} as n increases.[72] As a consequence the brightest peaks will be given by the following expression:

$$k_n=(2\pi/a)(F_{n-1}t^{-1}+F_{n-2})$$

obtained from (5) by replacing p and q by two successive Fibonacci numbers. Since t verifies the identity $t^{-n}=F_{n-1}t^{-1}+F_{n-2}$ (since $t^2+t=1$), this leads to

$$k_n=(2\pi/a)t^{-n}\ . \tag{7}$$

Expression (7) predicts that the peaks occur in geometrical progression with t^{-1} as the common ratio. In fact, this geometrical progression is valid for each order of diffraction and the general form of the expression of the wave vector corresponding to the strongest peaks is

$$k_{n,l}=(2\pi/a)lt^{-n} \tag{8}$$

with $n=0,1,2,\ldots$ and $l=1,2,\ldots$ In Fig. 3 this striking prediction is very clearly verified. We are able to identify, for example, the following families of peaks ($l=1$, $n=1-7$), ($l=2$, $n=1-6$), etc. In Fig. 4 we have plotted the measured ratios $k_{n+1,l}/k_{n,l}$ for these two families $l=1$ and $l=2$. We thus measure an "experimentally" determined golden mean $k_{n+1,l/k_{n,l}}=1.62\pm0.01$ (compared to the exact value $t^{-1}=1.6180\ldots$). From these data we can further determine the average lattice spacing. Since the whole angle interval which has been measured corresponds to 60°, we obtain a measured average spacing $a=17\pm1$ μm in good agreement with the theoretical value of 16 μm. This ±1 μm uncertainty is not caused by the errors in the position of the grooves (which are built with a much better precision of order ±0.05 μm) but only reflects the limited precision of the present optical diffraction measurements.

It is interesting to note that the spatial Fourier transform provides useful information on the spectrum. In the limit of very small scattering power, each scatterer scatters the wave only once, and the reflected wave can be obtained as the sum of the contribution of each scatterer. Due to the e^{ikr} dephasing of the wave during its propagation, the reflected wave is thus simply propor-

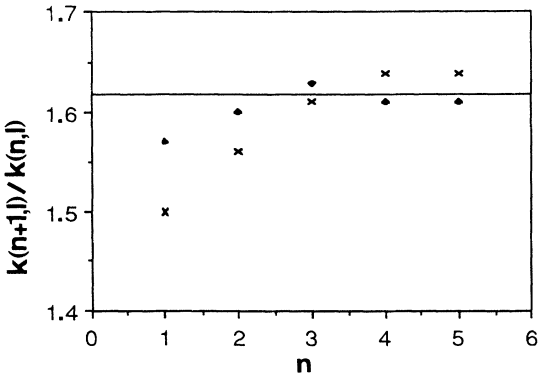

FIG. 4. Plot of the measured ratios $k_{n+1,1}/k_{n,l}$ for the two main families $l=1$ (crosses) and $l=2$ (black diamonds) shown in Fig. 3. This ratio gives an experimental determination of the inverse golden mean whose exact value is given by the horizontal line ($t^{-1}=1.61803\ldots$).

tional to the Fourier transform of the density of scatterers. This is the usual so-called Born regime. In this limit, the spatial Fourier transform and the spectrum described below should be indistinguishable. However, as soon as multiple scattering effects are present, the spatial Fourier transform and the spectrum become different. The spectrum then contains important contributions from paths having suffered multiple scattering. In this sense, the difference between the spectrum and the spatial Fourier transform of the system embodies the influence of multiple scattering. In a previous work[7] we have studied the spectrum of a special quasiperiodic system of grooves, obtained by the superposition of two periodic systems of periods P and Q, with $P/Q=t$, the golden mean. In this case one can show,[6] that due to its special structure, the spectrum is indeed equivalent to the spatial Fourier transform of the positions of the grooves along the system, even in the presence of multiple scattering. In the case of the quasiperiodic system studied here, this property is no longer true in a strict sense. However, there still exists an analogy. Both the spatial Fourier transform of the system and the spectrum can be understood on the basis of the decomposition of the whole system as a superposition of periodic systems of increasing periods, as will be explained in detail below.

C. The spectrum

1. Summary of some expected theoretical results

Let us first recall the expected properties of the spectrum. In order to understand the experimental results reported below, we use the transfer matrix theory presented in Appendix A describing the equation of propagation of SAW in presence of grooves which act as one-dimensional scatterers. Appendix A shows that the propagation of surface acoustic waves propagating on such a corrugated surface with grooves placed according to a Fibonacci sequence is equivalent to the propagation of electrons on a Fibonacci sequence of step potentials in a particular tight-binding model.

In particular, we learn from Refs. 26 and 33–47 that this system should be in the so-called "critical" regime intermediate between the extended and the localized regimes. For the spectrum, this means that gaps (or stop bands) are present at all frequency scales. Indeed, a generic feature of wave propagation in quasiperiodic systems, built recursively according to expression (1) or to some variants, is that their spectrum is a Cantor set of zero measure. The complementary set to the spectrum is the set of stop bands which thus covers densely the frequency range with the measure one. A Cantor set is special since it has zero measure but is undenumerable. This property puts these types of systems in between "extended" systems for which the spectrum is continuous and has a finite measure and "localized" systems for which the spectrum is "pure point," i.e., denumerable with zero measure. In an experiment, the observation of the Cantor structure of the spectrum is of course limited by the finite size of the system.

2. Description of the experimental results

Figures 5 and 7 represent different magnifications of the dependence of the transmission coefficient T as a function of frequency f obtained in our experiments. Figure 6 gives the experimental reflection coefficient on

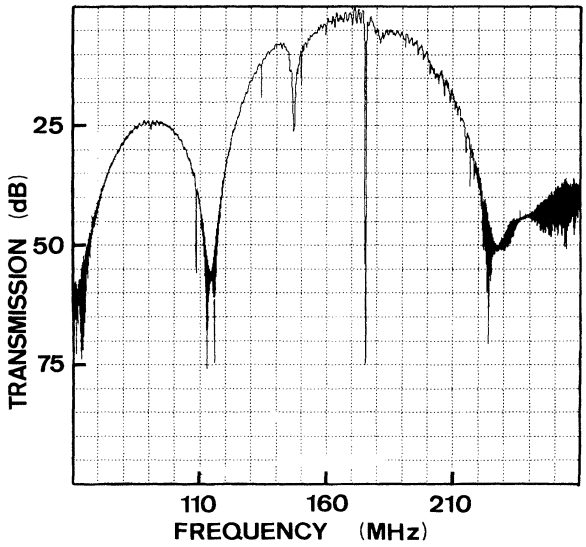

FIG. 5. General view of the SAW energy-transmission coefficient of a system containing 1000 grooves as a function of frequency over a large frequency interval. The large scale bell-like shape and secondary lobes correspond to the passing band and response of the transducers. The information relevant to the study of the quasiperiodic system is contained in the position and amplitude of the peaks which decorate the large-scale structure.

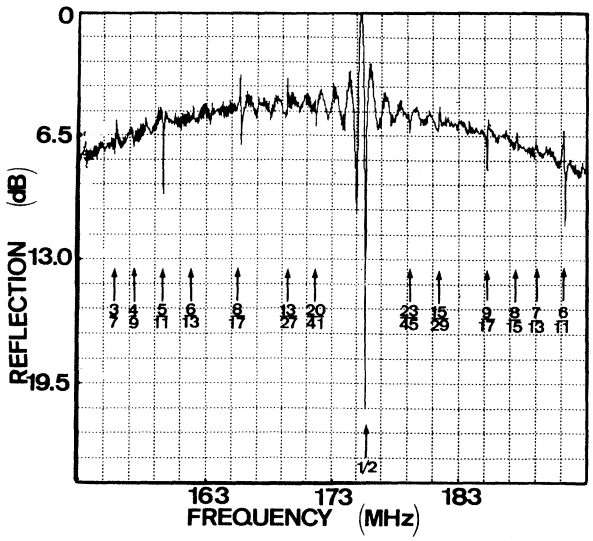

FIG. 6. Dependence of the SAW reflection modulus as a function of frequency. Each peak probes the existence of a stop band. The numbers under the arrows correspond to different values of the controlling parameter at/λ which is discussed in the text.

the same system as a function of frequency. The large-scale structure of the spectrum measured in reflection in Fig. 5 is characterized by three main lobes corresponding to the transfer function of the measuring transducers. The information relevant to the study of the $(d=1)$

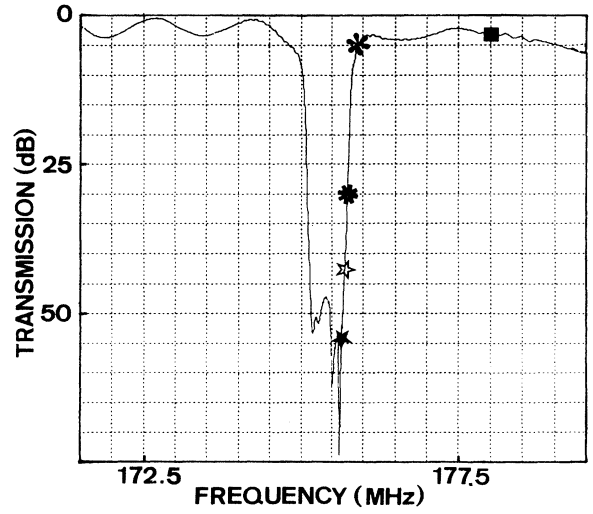

FIG. 7. Detail of the spectrum obtained in transmission showing the main gap corresponding to $at/\lambda=1/2$. The five different symbols decorating the right side of the gap corresponds to five frequencies at which the spatial structure of the SAW has been probed (see Ref. 2 and J. P. Desideri and D. Sornette, in preparation).

quasicrystal are the peaks which decorate this large-scale structure. The quality of the measurements is such that the signal-over-noise ratio is better than 80 dB.

We observe the existence of particular frequencies f for which the transmission coefficient is significantly decreased. This can be interpreted as the largest stop bands of the system. It is easy to verify in Fig. 5 that successive spacings in frequency between the main observed inverted peaks are in the ratio of the golden mean. In fact, the quasiperiodic structure of the lattice of grooves is reflected on the spectrum by a quasiperiodic system of inverted peaks. This observation can be extended at increasingly finer scales at which one verifies that the ratio of successive peak frequency spacings is a power of the golden mean. We thus recover on the spectrum the *self-similar* quasiperiodic structure of the system of grooves.

In Figs. 5 and 7 all peaks are inverted which corresponds to a decrease of the transmission. In Fig. 6 a decrease of transmission is associated with an increase of the reflection which explains the existence of positive peaks. However, note that, in general, peaks appear as negative-positive doublets in Fig. 6. This stems from the fact that the transducer which measures the reflected signals is different from the launching transducer and placed in between it and the system of grooves. For sufficiently large stop bands, there exists an interference between the reflected SAW and the direct wave propagation from the launching to the measuring transducer which produces a differential phase rotation leading to a sign change in a portion of the signal.

We note that the peaks in Figs. 5–7 in the neighborhood of the central frequency $f\approx 175$ Mhz can be indexed by a single integer n such that the variable at/λ is of the form

$$at/\lambda = n/(2n\pm 1) \quad n=1,2,\ldots\infty \ . \tag{9}$$

These series converge rapidly to $\frac{1}{2}$ as $n\rightarrow+\infty$. For instance, the central peak occurs for $0.4990\leq at/\lambda\leq 0.5010$ $[n=1$ of the series (9) with $at/\lambda=n/(2n-1)]$ corresponding to a frequency $f\approx 175$ Mhz and a wavelength $\lambda\approx 19.7$ μm. In Figs. 5 and 6 one can identify the different frequencies giving the smallest n for the rational expression (9) of at/λ:

$n=6$; $at/\lambda=\frac{6}{11}$; $f=191.35$ Mhz; $\lambda=18.12$ μm ,

$n=7$; $at/\lambda=\frac{7}{13}$; $f=189.35$ Mhz; $\lambda=18.35$ μm, etc .

We observe also a series of peaks in the frequency range for which a/λ, is in the neighborhood of $\frac{1}{2}$ and so on.

3. *Heuristic explanation of the experimental results*

First, let us give a heuristic rationalization of these results. In this goal we use the following essential property of the Fibonacci quasicrystal: it is the asymptotic limit of a series of periodic systems of larger and larger periods a_j, each corresponding to the successive "words" of the

iterative concatenation process (1). Let us now make explicit this point in some details. Consider the first smallest period a_0 corresponding to the complete pattern of letters "s" and "c." Since "s" ("c") occur with relative frequency $t/(t+1)$ $[1/(t+1)]$, a_0 is given by

$$a_0 = st/(t+1) + c/(t+1) \ . \tag{10}$$

Thus $a_0 \equiv a$, the average period of the system. We expect and observe a stop band at the Bragg condition $2a_0 = \lambda$, i.e., at a value of the reduced parameter $a/\lambda = \frac{1}{2}$.

The next smaller period a_1 is given by Eq. (10) with "s" replaced by "c" and "c" replaced by "sc," which gives $a_1 = t^{-1}a_0$. It is obtained from the self-similar structure of the quasicrystal which is invariant under the following transformation:

$$c \rightarrow s, \quad sc \rightarrow c \ , \tag{11}$$

which is illustrated in Fig. 2(b). One expects therefore a stop band indexed by the reduced parameter $a_1/\lambda = at^{-2}/\lambda = \frac{1}{2}$. The discussion is easily generalized to the larger periods $a_j = t^{-j}a_0$, obtained by replacing the word S_j by "c" and S_{j-1} by "s" in the infinite quasicrystal. This leads to gaps at frequencies such that

$$at^{-j}/\lambda = \tfrac{1}{2} \quad \text{with } j \geq 0 \ . \tag{12}$$

Expression (12) gives only a part of the whole spectrum. Indeed, it must be generalized to take account of the interactions between the different periods in the system. It is well known that, for any periodic system, there should be a gap at half of any reciprocal lattice vector $2\pi/b_j$ of the crystal, and all *sums* and *differences* of the reciprocal lattice vectors of the periodic structures are reciprocal lattice vectors. As the system becomes higher and higher order periodic (i.e., the integers become larger), the smallest reciprocal lattice vector of the system gets smaller and smaller. Thus, in the almost periodic limit, there should be a gap in the vicinity of every wave vector. This implies a highly fragmented Cantor-like band structure already discussed.

Now, consider the two reciprocal lattice vectors $2\pi/a_0$ and $2\pi/a_1$. Their sum is $(2\pi/a_0)(1+t) = 2\pi/a_0 t$ which is again a reciprocal lattice vector with $b = a_0 t$. The Bragg condition applied to it yields a gap for $a_0 t/\lambda = \frac{1}{2}$. This is the main gap observed experimentally in Figs. 5–7. Repeating the argument for the two reciprocal lattice vectors $2\pi/ta_0$ and $2\pi/a_0$ yields a reciprocal vector equal to $2\pi/a_0 t^2$, and so on. One thus generates gaps at all wavelengths for which Eq. (12) holds but with $j < 0$. These gaps are of course a few among the infinite set of the singular continuous spectrum. However, they are those which are the strongest, i.e., the largest since they correspond to successive periodic approximation of the quasicrystal with the *smallest* periods. The smallest periods will give the largest reflection and smallest transmission since this will correspond to the largest number of periods per unit length in the effective period lattice. Note that the series (14) with the smallest j's corresponds to the most favorable case and gives the strongest reflection coefficient and conversely the smallest transmission. This is well illustrated on our experimental and numerical results.

We are now able to understand the existence of the full series (9) observed experimentally. Until now we have considered only a combination of the fundamental reciprocal wave vector $2\pi/b$. Of course, if $2\pi/b$ is a reciprocal lattice vector, $2\pi/(2n\pm1)b$ reciprocal lattice vector since it corresponds to a period $(2n\pm1)b$ which is a multiple of the fundamental period b. Let us take $b = a$ and consider the following combination $2\pi/(2n\pm1)at^{-1} + 2\pi/(2n\pm1)a = 2\pi\{2n/(2n\pm1)\}/at$. The Bragg condition for this reciprocal lattice vector yields exactly the series (9). Such combinations of reciprocal vectors allows one to understand the peculiar role played by the frequencies such that at/λ is rational which have been observed experimentally.

This reasoning is confirmed by a direct numerical computation of the spectrum using the transfer matrix theory presented in Appendix A with the mapping approach of Kohmoto *et al.*[33,36,38–40] recalled and adapted to our system in Appendix B to the case of SAW propagation. In the computation we have used the following expression for ϕ_n:

$$\phi_n = (2\pi/\lambda)W_n \ , \tag{13}$$

where W_n is obtained from expression (2). In an infinite system, our results are comparable to previous ones obtained for quasiperiodic Schrödinger equations with a *step* potential,[33] since the transfer matrix formalism is the same in both cases. In our numerical computation we have taken an explicit account of the finite size N of the system and of the small value of the amplitude reflection coefficient μ. Figure 8 shows the effective finite-size spectrum as determined numerically from the mapping described in Appendix B, for $\mu = 0.01$. Stop bands (i.e., frequency intervals for which the transmission is significantly decreased) lie within vertical spaces surrounded by unconnected horizontal spaces: in other words, they are depicted as "gaps" in Fig. 8. Thick bars are due to close packing of such gaps. The apparent "finite-size" spectrum shown on Fig. 8 is obtained with the criterion that only those frequencies, yielding a value strictly larger than 2 for the trace of the transfer matrix for the whole system, are selected as "effective" stop bands. This criterion is a natural generalization of the simple periodic lattice case for which a passing band (stop band) is characterized by a value of the trace of the global transfer matrix less or equal to 2 (larger than 2). Note that we recover the main stop bands observed experimentally in the vicinity of the central band. These stop bands are indicated by the arrows with their corresponding values of the number at/λ.

This theory predicts not only a rich self-similar structure of the positions of the stop bands in the spectrum, but also that the depths of the stop bands are largely distributed. This is indeed observed in Figs. 5(a) and 5(b). A first qualitative rule of thumb is that a stop band is deeper when its frequency f is such that its corresponding value at/λ can be expressed as a rational number p/q with a small q. This property stems from the above

description of the quasicrystal as a superposition of periodic systems of increasing periods: the larger the number of periods in the relevant periodic system, the larger the attenuation when the corresponding Bragg condition is fulfilled (which occurs for a specific frequency). This is well observed for the special case $at/\lambda=\frac{1}{2}$, which corresponds to the smallest possible value of $q\neq 1$, for which an attenuation of 75 dB is measured on the system of 1000 grooves. The other stop bands seem to follow this rule in general, but important deviations are observed. For instance, the wide band around 147 mHz corresponds to a value $at/\lambda=\frac{5}{12}$, which gives a small q (and therefore a relatively large attenuation as expected). But, the attenuation measured at its center is significantly larger than those measured for stop bands around $at/\lambda=\frac{4}{9}$, which is in disagreement with the preceding rule of thumb (since $9<12$). Such deviations reveal that important interactions between the propagation wave and *several* equivalent periodic lattices are present, thus implying that the above rule of thumb is too simplistic to account for these effects. A quantitative understanding of this phenomenon requires the experimental study of systems of largely different sizes and a careful comparison with the numerical study of the dynamical system described above. We intend to come back to this problem in a future work.

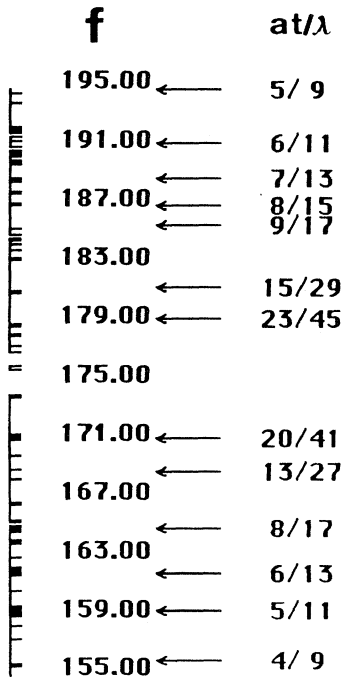

FIG. 8. Numerically determined finite-size spectrum obtained from the transfer matrix formalism described in the text and in Refs. 33 and 36–40 (see also Appendixes A and B). Stop bands lie within vertical spaces between unconnected horizontal bars. Thick bars are due to close packing of such gaps. Values of at/λ given by Eq. (9) are listed at the outmost right. The vertical list of equidistant frequencies in the middle gives the frequency scale. The comparison between Figs. 6 and 8 is good.

4. *Finite-size effects on the spectrum*

Looking at Figs. 5–8, it is clear that we do not observe the full Cantor structure predicted for the spectrum in an infinite system. Of course, this comes from the finite length of the system which contains (only) $N=1000$ grooves. Also, due to the fact that each groove is shallow ($h=0.3$ μm) compared to the typical value of the wavelength $\lambda\approx 20$ μm, and thus possesses a relatively small reflecting efficiency ($\mu\approx 10^{-2}$), the largest stop bands are rather narrow. If we note $\Delta\lambda_i$ the width of the ith gap, then we have $\Delta\lambda_i/a\leq 2\mu$ where μ is the amplitude reflection coefficient per groove.

Let us quantify more precisely the effect of the finite size of the system on the detection of stop bands. In the following argument we first note that a given frequency f will be detected as belonging to a stop band if and only if its transmission coefficient is not too close to one. In practice we fix a threshold stating that if the transmission is, say, 1 dB below the reference SAW signal, then the frequency qualifies as belonging to a stop band. We can generalize this criterion by choosing a different threshold, called t (for threshold in dB), for the decrease of the transmission measured in dB. The second step of the reasoning is to relate the transmission coefficient to the so-called Lyapunov exponent γ, which is nothing else than the inverse of the length ξ_γ of penetration of the wave inside the system. For the ith gap, the amplitude of the SAW decreases inside the system exponentially fast as $\Psi(x)=\Psi_0\exp\{-\gamma_i x\}$ with a characteristic decay equal to the Lyapunov exponent γ_i. Thus, for a system of length N, the transmission across it reads $T=T_0\exp\{-\gamma_i N\}$. This gives a decrease T (expressed in decibels) $=10(\log_{10}e)\,\gamma_i N=4.34\gamma_i N$ dB below the input signal. Remember that in our case, $\mu\leq 10^{-2}$ and $N=10^3$. The last step of the reasoning is to relate the value of the Lyapunov exponent γ_i to the observed width $\Delta\lambda_i$ of the ith stop band:

$$\gamma_i\approx\Delta\lambda_i/a\approx\epsilon_i\mu\ ,$$

where we note $\Delta\lambda_i/a=\epsilon_i\mu$ where $0\leq\epsilon_i\leq 1$. Using $\gamma_i\approx\epsilon_i\mu$, this yields T (dB)$=-43.4\epsilon_i$. Finally, the stop bands which can be detected in our experiments must satisfy the above criterion that T(dB) must be larger than t, which gives

$$\epsilon_i>\epsilon_0=0.23\ (\mu N)^{-1}t \approx 2.3\times 10^{-2}\ t,\quad \text{with } \mu\approx 10^{-2} \text{ and } N=10^3\ . \tag{14}$$

Choosing, for instance, $t\approx 1$ dB gives that only those stop bands possessing a width $\Delta\lambda$ larger than a few 10^{-2} μa can be detected in our experiments. This condition is stringent since only the gaps which have a width larger than the fraction ϵ_0 of the maximum possible width μ will be detected. This explains the experimental observation that most of the spectrum looks like a set of effective passing bands separated by small gaps. The special frequencies, which correspond to the surviving stop bands in the finite-size system, are those for which the transmis-

sion is small enough or conversely the reflection is large enough in order to be detected.

If the length of the experimental system is increased, the above estimation predicts that new stop bands will become visible. Indeed, expression (14) shows, for instance, that by doubling the number N of scatterers in the system, the smallest stop bands which can be detected possess a width which is half the width of the smallest detectable stop bands in the shorter system. As a consequence one expects to observe a much richer structure in the experimental spectrum when increasing the size of the system. This effect is clearly observed in Fig. 9 which compares the spectrum (transmission coefficient as a function of frequency) for two systems: the two figures on the left (right) correspond to a system having $N=1000$ (2000) grooves. The two figures at the bottom (which cover the frequency interval 140–160 MHz) show a magnified view of the two figures at the top (which cover the frequency interval 130–210 MHz). By comparison of the smaller and larger systems, one observes two interesting facts.

(1) The stop bands which were already present in the smallest system of $N=1000$ grooves are deeper and wider in the larger system of $N=2000$ grooves.

(2) Furthermore, a "cloud" of smaller stop bands appear in the larger system, which were not visible in the smaller system. This is particularly clear on the right side of the main stop band which can be observed on the

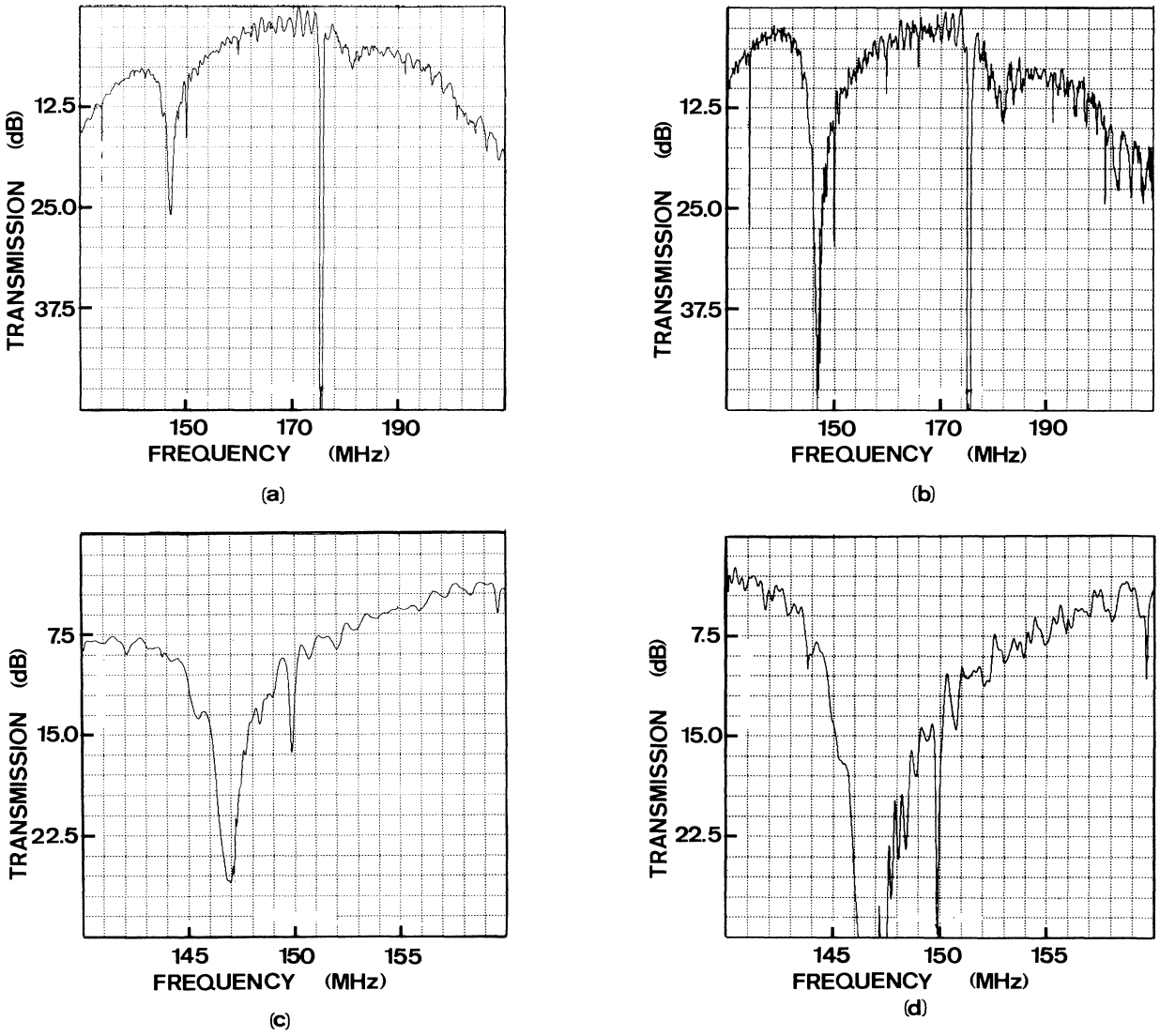

FIG. 9. Experimental spectra in the frequency interval 130–210 MHz measured for two systems of two different sizes constructed according to the Fibonacci sequence. (a) 1000 grooves; (b) 2000 grooves. (c) Gives a magnified view of the transmission coefficient presented in (a), in the interval 140–160 MHz; (d) is a magnified view of (b). The comparison between (a) and (b) [(c) and (d)] shows that enlarging the system produces two main effects: (1) gaps are deeper in the larger system; (2) new gaps appear in the larger system compared to the smaller one.

two figures at the bottom.

This observation is quite interesting because it is in agreement with our expectation that by increasing the size of the system, one should eventually tend toward a true Cantor spectrum, covered everywhere by a hierarchy of stop bands, each stop band possessing of course its own depth controlled by the period of the subsystem to which it corresponds.

In addition to suppressing a large fraction of the total number of stop bands in the spectrum, the finite size of our experimental system has another important consequence. The finiteness of the experimental system will also entail a smoothing of the stop bands corresponding to the finite number of digits used to represent the variable at/λ. This can be best seen within the approximation introduced in Ref. 2 which amounts to replacing the exact expression (10) for ϕ_n by the approximation

$$\phi_n = 2\pi \,\mathrm{frac}\{nat/\lambda\} \ .$$

With this approximation, the structure of the spectrum can be understood qualitatively from successive principal convergents of the irrational number at/λ. This formulation is particularly suitable to analyze precisely the finite-system size effect. Indeed, in a system of $N=1000$ grooves, the denominator q of the rational approximation to at/λ cannot be greater than $\sim N/2$ since a finite system of length n corresponds approximately to a periodic system of maximum period $\sim N/2$. This means that at/λ can be experimentally considered as an irrational only if the following condition is verified: consider the two successive rational approximations of at/λ, say p/q and p'/q'. These two successive rational approximations are experimentally distinguishable if and only if q and q' are both less than $\sim N/2$. Let us therefore consider a given value of the SAW frequency such that $at/\lambda = p/q$ with $q \leq N/2$ corresponding to a given finite continued fraction expansion of the form

$$\cfrac{1}{r_1+\cfrac{1}{r_2+\ddots\cfrac{1}{r_n}}} \ .$$

Let us then consider the set of rationals close to p/q of the form

$$\cfrac{1}{r_1+\cfrac{1}{r_2+\ddots\cfrac{1}{r_n+\cfrac{1}{x}}}}$$

with $x = 1, \ldots, \infty$. Transforming this truncated continued fraction to a rational p'/q', we determine x such that $q' \sim N/2$. Then p' is easily obtained and the difference $p'/q' - p/q$ gives the interval in at/λ over which the problem is equivalent to the propagation of a SAW on a periodic lattice of period q.

Let us treat in detail the case when $at/\lambda = 0.5$. The measured width of this stop band is $\Delta f = 0.6 \pm 0.1$ Mhz yielding $\Delta f/f \approx (3.5 \pm 0.5) \times 10^{-3}$. The theoretical value corresponds to the two λ's such that $(1+\mu^2/2)\cos 2\pi at/\lambda = 1$ which gives $\Delta f/f_{\text{theor}} \approx 3 \times 10^{-3}$ in reasonable agreement with the experimental value, considering the imprecision of the measure of the stop-band width. For this band we can estimate the size of the frequency interval over which the system is equivalent to a periodic system of period $2a$. In the case $p/q = \frac{1}{2}$, we have $r_0 = 0$, $r_1 = 1$, and $r_2 = 1$. Then, $x = 249$, which yields $p'/q' = 250/499 = 0.5010$, roughly corresponds to the measured width of the stop band $p/q - p'/q' \sim 10^{-3}$. Note that this last result is just another way of quantifying the stop-band width. In this case, the width and rounding due to finite-size effects are in fact of the same order. For other stop bands which are predicted to be smaller, their observed width is thus limited by the finite-size rounding effect. Note that for another rational number with a higher value of q, for example, $at/\lambda = 9/17$, we have $r_0 = 0$, $r_1 = 1$, $r_2 = 1$, and $r_3 = 8$. This allows us to obtain $x = 29$ and $p'/q' = 262/495 \approx 0.5293$. In this case, $p/q - p'/q' \sim 10^{-4}$ which is much smaller than for $p/q = 1/2$ and not measurable since the stop band is smaller than the experimental spectral resolution.

5. *Analysis of the impulse response*

The information in the time domain is in principle equivalent to that obtained from the spectrum discussed in Sec. III C since it is obtained from it by a simple Fourier transform. We have verified this point in our experiments: the impulse response obtained experimentally is indistinguishable from the numerical Fourier transform of the experimentally determined frequency spectrum. However, it gives a nice complementary picture of the SAW propagation which may be in some cases more intuitive. Certain features are much clearer in the time domain. For instance, it can be very useful for locating the position of the scatterers or at least, if the time resolution is not sufficient, for obtaining gross features of the system by focusing on the time patterns.

With a central frequency of $\langle f \rangle = 173$ Mhz with a 20% bandwidth, we expect a minimum width of the pulse of the order of $\Delta t \approx 1.4 \times 10^{-2}$ μs corresponding to a spatial width $\Delta d \approx 50$ μm for a SAW group velocity $c \approx 3470$ m/s. Knowing precisely the length $L = 15\,984$ μm of the system and measuring the time delay for the pulse to reach the last groove and come back to the emitting transducer, we measure the Rayleigh SAW group velocity $c = 2L/(t_1 - t_0)$ with $t_1 - t_0 = 9.20 \pm 0.02$ μs and obtain $c = 3473 \pm 6$ m/s which is in good agreement with the expected value for lithium niobate at room temperature.[74]

Figure 10 presents the SAW intensity emitted by the launching transducer and received under reflection on the receiving transducer as a function of time, over the whole time span for which a useful signal larger than the noise can be detected. Both transducers are placed on the left of the system and the launching transducer is the farthest

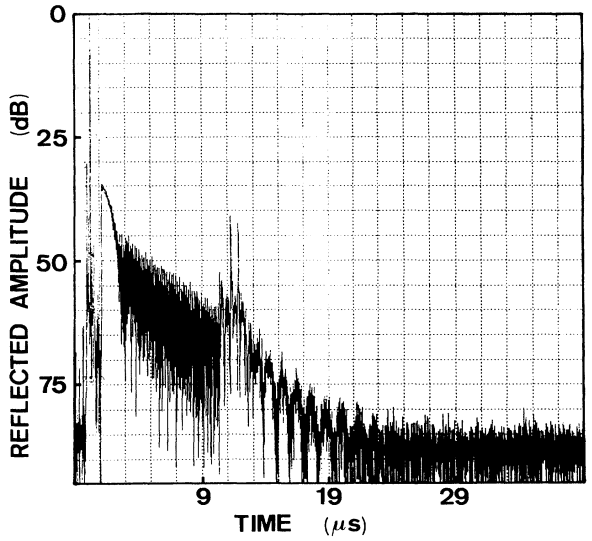

FIG. 10. Large-scale time-impulse response under reflection on the quasiperiodic system. The encounter with the first groove corresponds to the time $t_1 = 1.15$ μs counted from the launching time. This origin corresponds to the highest peak occurring just before the reference peak at zero dB on the figures (see text).

away on the left. The SAW propagates from left to right before being reflected by the system of grooves. The encounter with the first groove corresponds to the time $t_1 = 1.15$ μs counted from the launching time. This origin corresponds to the electromagnetic signal radiated from the launching transducer and which has propagated at the velocity of light to the receiving transducer. Compared to sound velocity, the light velocity is as if infinite and thus marks the origin of time. Just behind this electromagnetic radiated signal, one observes a peak at zero dB on the figures which corresponds to the direct transmission of the SAW from the launching to the receiving transducer. The length ct_1 corresponds to the distance from the launching transducer to the first reflecting groove and from it back to the reflecting transducer. We measure a reflected SAW signal around -35 dB below the incident SAW. In order to understand this measure we propose the following explanation. Let us consider that at any time the pulse of spatial extension ~ 50 μm covers roughly three grooves since $3a = 48$ μm. Assuming an energy reflection $\approx \mu^2$ per groove, the total signal for the incoherent reflection over three grooves is $10 \log_{10} 3\mu^2 = -36$ dB, taking $\mu \approx 9 \times 10^{-3}$ for the central frequency. This is in good agreement with the measured value.

Up to the time ≈ 10 μs we measure essentially the contribution from paths involving simple reflection. Beyond this time we observe paths involving triple reflections on three different grooves of the system. The high peaks at times $\approx 11-12$ μs correspond to the reflection of the SAW on the transducer placed on the right of the system which is used in transmission measurements.

The most distinctive feature of Fig. 11 is the transition from a regime at times less than ≈ 2.4 μs for which the impulse response is roughly a monotonously decreasing function of time to the regime at larger times where a well-ordered pattern of peaks appears corresponding to a

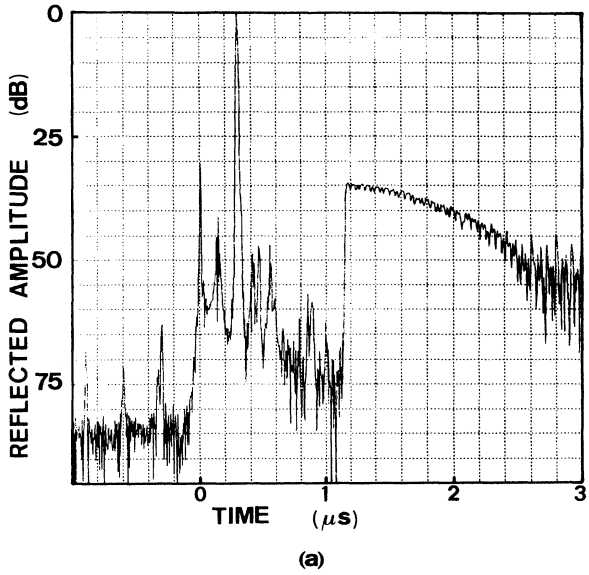

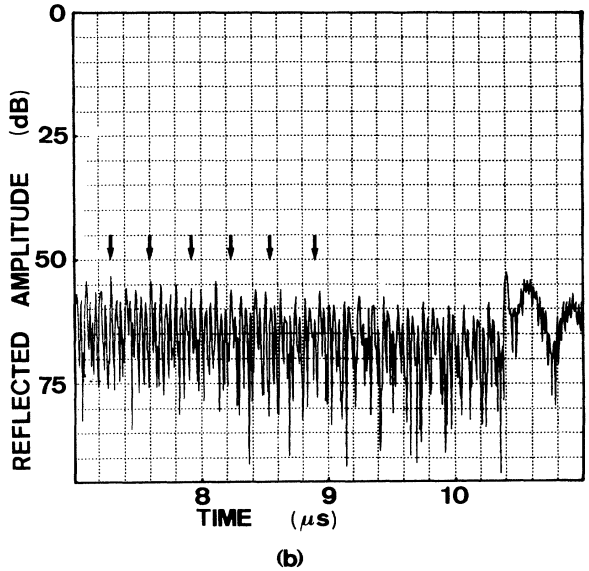

FIG. 11. Details of the time impulse response under reflection shown in Fig. 10. The SAW is launched from one transducer ($T1$) at the left of the system and is received by a second transducer ($T2$) placed in between the transducer ($T1$) and the system. (a) The time impulse response at short times is shown. Note the transition from a regime at times less than ≈ 2.4 μs (the time $t = 0$ is the origin of time at which the pulse has been launched) for which the impulse response is roughly monotonous to the regime at larger times where a well-ordered pattern of peaks appears, as shown in (b). (b) This figure shows the last single reflections on an individual groove or small groups of grooves and the transition to a triple reflection regime at long times $t \geq 10.4$.

quasiperiodic temporal dependence. This transition can be explained from a competition between the reflection by different families of subsystems of increasing periods in the quasiperiodic system. The first regime corresponds to the reflection over an effective periodic lattice of minimal period "a." This contribution decreases typically over a distance of the order a/μ. Therefore, beyond a time $\Delta t \approx a/c\mu$, we will begin to observe the contribution to the reflection stemming from larger periodic subsystems. We can alternatively associate the duration Δt of this first regime with the inverse $1/\Delta f$ of the width Δf of the central peak at $at/\lambda = 1/2$. We have estimated it above from the measured spectrum and also theoretically. Indeed, the measured width of this stop band is $\Delta f = 0.6 \pm 0.1$ Mhz and the theoretical value corresponds to the two closest λ's such that $(1+\mu^2/2)\cos 2\pi at/\lambda = 1$ which gives $\Delta f = (c/\pi at)\mu \approx 0.5$ MHz. Thus, $\Delta t \approx 1.7-2$ μs which is well in agreement with the observed duration of the first regime on Fig. 11(a).

Beyond this regime we can identify several families of peaks. Each family is characterized by a periodic separation but a nonconstant intensity. The family pointed out by the arrows in Fig. 11(b) corresponds to a periodic time delay of 0.314 μs between each successive peak, i.e., to a distance $2d \approx 1088 \pm 10$ μm traveled by the SAW. Each peak of this family corresponds therefore to a reflection upon a groove (or a small set of grooves) separated by the constant distance $d = 544 \pm 5$ μm. But, this is precisely equal to $F_8 a = 544$ μm with $F_8 = 34$ and $a = 16$ μm. This gives the clue to search for different periodicities of the form $F_j a$ with $j = 4, 5, 6, \ldots$. Indeed, we can identify the family $F_6 = 13$ by a measured separation of 210 ± 5 μm in good agreement with $F_6 a = 208$ μm. For $F_7 = 21$, the measured separation is 340 ± 5 μm which compares well with $F_7 a = 336$ μm. And so on.

The appearance of the different periods $F_4 = 5$, $F_5 = 8$, $F_6 = 13$, $F_7 = 21$, $F_7 = 21$, $F_8 = 34$, $F_9 = 55$, $F_{10} = 89$, $F_{11} = 144, \ldots$, can be explained as follows. Consider, for example, the successive words of 5 letters such as "*scssc*," "*sscsc*" which appear in the Fibonacci sequence (1). One observes that each such word always contains three "*s*" and two "*c*" and even if the ordering is different, the total length of the 5-word is always equal to $3s + 2c$. This shows the existence of the period $F_4 = 5$ in the system. The argument also holds for all successive Fibonacci numbers and this explains the observed highly structured pattern. The fact that for a given family, say F_8, we observe four subfamilies having the same period but with different origins and intensities could be explained by the fact that each reflection stems from the contribution of three grooves (due to the finite pulse duration which overlaps over three grooves) and only four different ordering of three letters appear in the quasicrystal which are "*scs*," "*css*," "*ssc*," and "*csc*." To each ordering corresponds a given reflection intensity which controls the amplitude of the corresponding subfamily.

In the large time domain, the reflected pulses have an intensity decreasing approximately exponentially with time (we observe a linear envelop in the logarithm of intensity as a function of time in Fig. 10). This allows us to extract the value of the SAW attenuation. Since the intensity is decreased by 8.2 dB over a time scale of 4 μs, we obtain a characteristic attenuation time of $2l_a/c = 1.97 \pm 0.09$ μs. This is in remarkable agreement with the value $l_a/c = 0.98 \pm 0.05$ μs determined by a direct measurement of the spatial decay of the SAW along the system, reported in Ref. 75.

IV. CONCLUSION

We have presented precise experimental results and their interpretation on the propagation of surface acoustic waves propagating at the surface of a quasiperiodically corrugated solid surface. The surface was made of one or two thousand grooves engraved according to a Fibonacci sequence. This type of one-dimensional system has been much studied theoretically in the literature in the context of electronic or phonon propagation. It exhibits many interesting transport features which recall some properties of strongly disordered systems related to Anderson localization. We have reported precise results about the reflection and/or transmission frequency dependence and the temporal impulse response of the systems. The propagation on the "quasicrystal" corresponds to a critical regime of the localization transition and we have given an experimental characterization of the critical structure of the spectrum. We have shown that its structure can be simply interpreted in terms of successive approximation of the quasicrystal by periodic subsystems of increasing periods.

These experimental results can be considered as preliminary tests before undertaking the analysis of completely disordered systems with their pure point spectrum, completely localized proper modes, and long tail characteristic time response. We will report on this problem in a future work.

ACKNOWLEDGMENTS

One of us (D.S.) acknowledges illuminating discussions with Dr. O. Legrand which helped him understand the structure of the spectrum and thank him for providing Fig. 8 We are grateful to J. F. Gelly and C. Maerfeld for their kind welcome in the DTAS Department of Thomson-Sintra at Sophia-Antipolis where the experiments have been carried out. We acknowledge financial support from DRET under Contract No. 86/177 for the research program "Propagation acoustique en milieux aléatoires." Laboratoire de Physique de la Matière condensée is a CNRS URA 190.

APPENDIX A

In this appendix we establish the connection between the SAW propagation on a corrugated surface and the tight-binding discrete Schrödinger model for electronic transport in a random or quasiperiodic potential.

1. The SAW transfer matrix

Since $(d=1)$ systems are always topologically ordered,[10] the equations for wave propagation in any $(d=1)$ system at any energy or frequency can be cast into essentially the same transfer matrix formalism. This is true as long as reactive effects or long-range interactions between neighboring (and sometimes distant) scatterers can be neglected. Then, such a formalism is able to predict the effect of dissipation, coherent losses (surface to bulk detrapping), and energy storage at the border of the grooves (due to the existence of evanescent waves) on the propagation properties of the arrays. Considering symmetric scatterers and a local energy flux conservation, we obtained in a previous work[70] the general form of the single symmetric scatterer transfer matrix for $(d=1)$ guided waves. It depends on four real parameters. Two among the four parameters of the transfer matrix have a simple meaning [similar to that for symplectic matrices,[1] one being related to the reflection coefficient of the scatterer and the other to the typical longitudinal scale of the $(d=1)$ scatterer]. The two other parameters describe the coupling of the guided SAW with the leaky bulk waves which corresponds to a kind of "coherent" attenuation.

In a first analysis, let us neglect the role of this leakage. This will simplify the theoretical modeling and allow us to exhibit the salient features of the systems. We will verify directly on the experiments the validity of this simplification, namely, that the leakage does not change significantly the predictions on the spectrum obtained by neglecting it. Then, the transfer matrix across a single space-symmetrical groove is symplectic and depends on two parameters.

To be concrete, let us consider a wave amplitude at point x of the general form: $Y_1(x)=Y_1^+e^{ik(x-x_0)}+Y_1^-e^{-ik(x-x_0)}$ before the scatterer and $Y_2(x)=Y_2^+e^{ik(x-x_0)}+Y_2^-e^{-ik(x-x_0)}$ after the scatterer which is located at $x=x_0$. The general expression of the matrix T is given by

$$\begin{bmatrix} Y_{n+1}^+ \\ Y_{n+1}^- \end{bmatrix} = T_n \begin{bmatrix} Y_n^+ \\ Y_n^- \end{bmatrix} = \begin{bmatrix} e^{i\phi_n} & 0 \\ 0 & e^{-i\phi_n} \end{bmatrix} \begin{bmatrix} a_n & b_n \\ c_n & d_n \end{bmatrix} \begin{bmatrix} Y_n^+ \\ Y_n^- \end{bmatrix} . \tag{A1}$$

In the absence of leakage, symmetry under time reversal imposes $d=a^*=(1-b)e^{i\alpha}$ and $c=b^*$.[70] We consider the case of inefficient or "small" scatterers such that the typical value of the reflection coefficient for a single scatterer is small. This is not a restriction since most situations fall into this class. Since $1/d=\{(1-b)e^{-i(\phi+\alpha)}\}^{-1}$ is the amplitude transmission coefficient, one expects $|1/d|\approx 1$ which implies $|b|\ll 1$ and $\alpha\ll 1$. ϕ has the meaning of a pure propagation dephasing. In a lattice of scatterers whose centers are positioned on $\{x_n\}$, $\phi_n=k(x_{n+1}-x_n)$ is the dephasing over the distance separating the $(n+1)$th from the nth groove and $|b/d|^2\approx\mu^2$ is the energy reflection coefficient. The amplitude reflection coefficient is μ. The transfer matrix T thus reads in this limit

$$T_n = \begin{bmatrix} \alpha_n=e^{i\phi_n}(1+i\mu_n) & \beta_n=i\mu_n e^{i\phi_n} \\ \beta_n^*=-i\mu_n e^{-i\phi_n} & \alpha_n^*=e^{-i\phi_n}(1-i\mu_n) \end{bmatrix} . \tag{A2}$$

To be concrete, consider the case of a Rayleigh SAW of wavelength $\lambda=2\pi/k$ propagating at the surface of a solid and impinging upon a groove of width w and depth h [see Fig. 1(b)]. A perturbative-type theory of the single scattering event,[64–68] confirmed by experimental measurements,[69] shows that a portion μ^2 of the energy of the wave is reflected and a portion p is converted to bulk longitudinal and shear waves. $\mu^2/p\approx 1/20$ with $\mu=0.6\,(h/\lambda)\sin(2\pi w/\lambda)$ (Refs. 31 and 64–69) where h/λ plays the role of the small parameter [$\mu\approx h/\lambda$ and $p\approx 20(h/\lambda)^2$]. Typically, $h\leq 1$ μm and $\lambda\geq 10$ μm leading to h/λ and μ in the range 10^{-1}–10^{-3}. For typical values $h=0.3$ μm, $w=5$ μm, and $f\approx 170$ Mhz with a SAW group velocity of the order of 3470 m/s leading to a wavelength $\lambda\approx 20.4$ μm, we obtain $\mu\approx 9\times 10^{-3}$ μm.

2. Correspondence with the Anderson tight-binding model

It is a very general result that one-dimensional wave or Schrödinger continuous equations as well as 2×2 transfer matrix equations can be transformed exactly onto a discrete (tight-binding) form.[10] This correspondence may be useful in order to relate our particular system to a large class of problems already studied in other contexts.

In our case we note $Y_n=Y_n^++Y_n^-$ the value of the SAW amplitude just before the nth scatterer (groove). From the transfer matrix equation (A1) written for $n\rightarrow n+1$, we obtain Y_{n+1} as a function of Y_n^+ and Y_n^-. Since the matrices T_n are unimodular, they are easily inverted with $T_n^{-1}=T_n^*$. This allows us to write $Y_{n-1}=Y_{n-1}^++Y_{n-1}^-$ as a function of Y_n^+ and Y_n^- by using Eq. (A1) for the transfer from $n-1$ to n. Solving for Y_n^+ and Y_n^- as a function of Y_{n+1} and Y_{n-1} gives $Y_n=Y_n^++Y_n^-$ as a function of Y_{n+1} and Y_{n-1} and thus the following off-diagonal tight-binding equation:

$$t_{n+1}Y_{n+1}+t_{n-1}Y_{n-1}-E_nY_n=0 \tag{A3}$$

with

$$\begin{aligned} t_{n+1}&=(\alpha_{n-1}-\alpha_{n-1}^*)-(\beta_{n-1}-\beta_{n-1}^*)\,, \\ t_{n-1}&=(\alpha_n-\alpha_n^*)-(\beta_n-\beta_n^*)\,, \\ E_n&=(\alpha_n+\beta_n^*)(\alpha_{n-1}-\beta_{n-1}) \\ &\quad -(\alpha_n^*+\beta_n)(\alpha_{n-1}^*-\beta_{n-1}^*)\,. \end{aligned} \tag{A4}$$

With the values of α_n and β_n given by Eq. (A2), this yields the following equation governing the SAW propagation over the groove array:

$$(\sin\phi_{n-1})Y_{n+1}+(\sin\phi_n)Y_{n-1} -[\sin(\phi_{n-1}+\phi_n)-2\mu\sin\phi_{n-1}\sin\phi_n]Y_n=0\,. \tag{A5}$$

We have used the fact that in our systems $\mu_n=\mu$ is in-

dependent on n and that the inhomogeneous (quasiperiodic) modulation enters only via the phases $\phi_n = k(x_{n+1} - x_n)$. By changing the physical parameter at our disposal, namely, the SAW frequency, we change k and therefore the ϕ_n and also the "energy" $E = \sin(\phi_{n-1} + \phi_n) - 2\mu \sin\phi_{n-1} \sin\phi_n$. This means that we are not studying a given tight-binding Schrödinger equation as a function of its eigenenergies but, in contrast, look at the evolution of the response of a succession of different tight-binding Schrödinger equations with a particular energy, one for each value of the wavelength.

APPENDIX B

1. *Theory for the propagation of SAW on the quasicrystalline lattice of grooves*

In the quasicrystal case considered in Sec. III, $\phi_n = k(x_{n+1} - x_n)$ represents the modulation of the groove position around their mean separation a. ϕ_n therefore takes two values $\phi_c = kc$ and $\phi_s = ks$ which occur following the Fibonacci sequence given by Eq. (1), i.e., with frequency $p(\phi_c) = t$ and $p(\phi_s) = t^2$ [we verify that $p(\phi_c) + p(\phi_s) = 1$ since t is the inverse golden mean]. Note that ϕ_n can be coded by formula (2) given in the text.

In order to describe the propagation of SAW on the quasicrystalline lattice of grooves we use the transfer matrix formalism introduced in Appendix A 1. We follow Kohmoto *et al.*[33,36–40] and consider the SAW propagation through the Fibonacci multigrooved system S_j constituted of F_j grooves. The SAW propagation over the distance s (c) is described by the corresponding transfer matrix $T_{s(c)}$. For the sequence $S_0 = \{s\}$, the total transfer matrix is $M_0 = T_s$. For $S_1 = \{c\}$, $M_1 = T_c$. For $S_2 = \{sc\}$, $M_2 = T_s T_c$, etc. Due to the simple recurrence equation for the $\{S_j\}$, the corresponding transfer matrix M_j obeys the simple recursion relation

$$M_j = M_{j-2} M_{j-1} . \tag{B1}$$

This equation is the same as the renormalization-group equation for a quasiperiodic Schrödinger equation with a *step* potential which has been extensively studied in Refs. 33 and 36–40. It can be considered as a dynamical map in a three-dimensional space (u_{j-1}, u_j, u_{j+1}) when expressed in the reduced variable $u_j = (\frac{1}{2})\,\mathrm{trace}\,(M_j)$:

$$u_{j+1} = 2u_j u_{j-1} - u_{j-2} . \tag{B2}$$

The map (B2) possesses a constant of motion

$$I = u_{j+1}^2 + u_j^2 + u_{j-1}^2 - 2u_{j+1} u_j u_{j-1} - 1 \tag{B3}$$

which means that the motion of a representative point (u_{j-1}, u_j, u_{j+1}) remains on a two-dimensional surface defined by Eq. (B3). In our case we obtain from expression (A2) that

$$u_0 = (\alpha_2 + \alpha_2^*)/2 = (1+\mu^2)^{1/2} \cos[\phi_s + \varphi(\mu)] ,$$

$$u_1 = (\alpha_1 + \alpha_1^*)/2 = (1+\mu^2)^{1/2} \cos[\phi_c + \varphi(\mu)] ,$$

$$u_2 = (1+\mu^2)^{1/2} \cos[\phi_c + \phi_s + 2\varphi(\mu)] + \mu^2 \cos(\phi_s - \phi_c) ,$$

where the phase $\varphi(\mu)$ is defined by $\tan\varphi(\mu) = \mu$. We thus obtain

$$I = \mu^2 \{ \sin^2[\phi_s + \varphi(\mu)] + \sin^2[\phi_c + \varphi(\mu)] - 2 \sin[\phi_s + \varphi(\mu)] \sin[\phi_c + \varphi(\mu)] \cos(\phi_s - \phi_c) \} + O(\mu^4) . \tag{B4}$$

For deriving Eq. (B4) we have used the identity $\alpha_1^2 + \alpha_2^2 + \alpha_3^2 - 2\alpha_1\alpha_2\alpha_3 - 1 = 0$ for $\alpha_{1,2,3} = \cos(\phi_{1,2,3})$ provided $\phi_3 = \phi_1 + \phi_2$. The constant of motion I represents the strength of the effect of quasiperiodicity and it is therefore reasonable that it should be proportional to μ^2. It also determines the size of the band gaps. A large I implies a large gap and $I = 0$ implies a vanishing gap. I vanishes for certain values of the SAW frequency indicating that in this case the effect of quasiperiodicity is not important.

Since u_j represents half the trace of the matrix M_j, it describes the spectrum of the commensurate problem with a unit cell of length $F_j a$. If $|u_j| < 1$ for a given frequency, this frequency lies in a band whereas if $|u_j| > 1$, it is in a gap. As $j \to +\infty$, for most frequencies, u_j will escape to infinity and then certainly $|u_j|$ will become greater than unity. Thus, most energies lie in a gap. We have used this property to determine the finite-size spectrum described in the text. More information can be found in Refs. 33 and 36–40.

As a final comment on this approach we note that Kohmoto *et al.* have considered a similar problem in which optical layers are constructed following the Fibonacci sequence. However, they consider the case in which the dephasing $\phi_c = \phi_s = \phi$ and $\mu_1 \neq \mu_2$. In this case, the value $\phi = (m + 1/2)\pi$, corresponding to a $\lambda/4$ matching, plays a special role since the map (B3) has a six cycle, namely, $M_j = M_{j+6}$ for any j. This implies that the transmission coefficient T has a rich scaling structure around $\phi = (m + 1/2)\pi$. These features do not appear to be present in our case due to the other choice $\phi_c \neq \phi_s$ and $\mu_1 = \mu_2 = \mu$.

*Present address: 63, Avenue de la Liberté, Golfe-Juan, 06220 Vallauris, France.

[1]B. Souillard, in *Chance and Matter,* NATO ASI Les Houches Summer School, Session XLVI, 1986, edited by J. Souletie, J. Vannimenus and R. Stora (North-Holland, Amsterdam, 1987); D. Sornette, Acustica **67**, 199 (1989); **67**, 251 (1989); **68**, 15 (1989).

[2]J. P. Desideri, L. Macon, and D. Sornette, Phys. Rev. Lett. **63**, 390 (1989).

[3]S. Tamura and F. Nori, Phys. Rev. B **40**, 9790 (1989); Q. Niu and F. Nori, Phys. Rev. Lett. **57**, 2057 (1986).

[4]L. S. Levitov, J. Phys. (Paris) **50**, 707 (1989).

[5]H. Hiramoto and M. Kohmoto, Phys. Rev. Lett. **62**, 2714 (1989); Phys. Rev. B **40**, 8225 (1989).

[6]J. Peyraud and J. Coste, Phys. Rev. B **37**, 3979 (1988).

[7]L. Macon, J. P. Desideri, and D. Sornette, Phys. Rev. B **40**, 3605 (1989).

[8]P. W. Anderson, Phys. Rev. **109**, 1492 (1958).

[9]D. Thouless, in *Ill-Condensed Matter,* edited by R. Balian, R. Maynard, and G. Toulouse (North-Holland, Amsterdam, 1979), pp. 1–62; K. Ishii, Suppl. Progr. Theor. Phys. **53**, 77 (1973); P. W. Anderson, D. J. Thouless, E. Abrahams, and D. S. Fisher, Phys. Rev. B **22**, 3519 (1980).

[10]J. M. Ziman, *Models of Disorders, the Theoretical Physics of Homogeneously Disordered Systems* (Cambridge University Press, Cambridge, England, 1979).

[11]E. Guazzelli, E. Guyon, and B. Souillard, J. Phys. Lett. (Paris) **44**, 837 (1982); M. Belzons, P. Devillard, F. Dunlop, E. Guazzelli, O. Paradi, and B. Souillard, Eur. Phys. Lett. **4**, 909 (1987).

[12]C. Hodges, J. Sound Vib. **82**, 411 (1982); V. Baluni and J. Willemsen, Phys. Rev. B **31**, 3358 (1985); T. R. Kirkpatrick, *ibid.* **31**, 5746 (1985); C. H. Hodges and J. Woodhouse, J. Acoust. Soc. Am. **74**, 894 (1983).

[13]C. Depollier, J. Kergomard, and F. Laloe, Ann. Phys. (Paris) **11**, 457 (1986).

[14]S. He and J. D. Maynard, Phys. Rev. Lett. **57**, 3171 (1986).

[15]D. T. Smith, C. P. Lorenson, R. B. Hallock, K. R. McCall, and R. A. Guyer, Phys. Rev. Lett. **61**, 1286 (1988); for the theoretical treatment, see S. M. Cohen and C. Machta, *ibid.* **54**, 2242 (1985); C. A. Condat and T. R. Kirkpatrick, Phys. Rev. B **33**, 3102 (1986); S. M. Cohen, J. Machta, T. R. Kirkpatrick, and C. A. Condat, Phys. Rev. Lett. **58**, 785 (1987).

[16]P. W. Adams and M. A. Paalanen, Phys. Rev. Lett. **61**, 451 (1988).

[17]E. Akkermans, P. E. Wolf, and R. Maynard, Phys. Rev. Lett. **56**, 1471 (1986).

[18]A. Ladendijk, M. P. Van Albada, and M. B. Van der Mark, Physica **140A**, 183 (1986).

[19]A. Z. Genack, Phys. Rev. Lett. **58**, 2043 (1987).

[20]T. R. Kirkpatrick and J. R. Dorfman, in *Fundamental Problems in Statistical Mechanics,* edited by E. G. D. Cohen (Elsevier, New York, 1985), Vol. VI.

[21]P. Sheng and Z. Q. Zhang, Phys. Rev. Lett. **57**, 1879 (1986); C. A. Condat and T. R. Kirkpatrick, *ibid.* **58**, 226 (1987).

[22]K. Arya, Z. B. Su, and J. L. Birman, Phys. Rev. Lett. **57**, 2725 (1986).

[23]D. Schechtman, I. Blech, D. Gratias, and J. W. Cahn, Phys. Rev. Lett. **53**, 1951 (1984).

[24]S. Aubry and C. André, in *Proceedings of the Israel Physical Society,* edited by C. G. Kuper 3 (Adam Hilger, Bristol, 1979), p. 133.

[25]Y.-Y. Zhu, N.-B. Ming, and W.-H. Jiang, Phys. Rev. B **40**, 8536 (1989); A. Wixforth, J. Scriba, M. Wassermeier, and J. P. Kotthaus, *ibid.* **40**, 7874 (1989).

[26]J. B. Sokoloff, Phys. Rep. **126**, 189 (1985).

[27]M. Ya. Azbel, Zh. Eksp. Teor. Fiz. **17**, 980 (1963) [Sov. Phys. JETP **17**, 665 (1963)]; **19**, 929 (1964) [**19**, 634 (1964)].

[28]L. B. Coleman, M. J. Cohen, D. J. Sandman, F. G. Yagamishi, A. F. Garito, and A. J. Heeger, Solid State Commun. **12**, 1125 (1973).

[29]M. J. Rice, A. R. Bishop, J. A. Krumhansl, and S. E. Trullinger, Phys. Rev. Lett. **36**, 432 (1976).

[30]C. K. Chiang, R. Spal, A. Denenstein, A. J. Heeger, N. D. Miro, and A. G. MacDiarmid, Solid State Commun. **22**, 293 (1977).

[31]E. A. Ash and E. G. S. Paige, in *Rayleigh-Wave Theory and Application,* Springer Series on Wave Phenomena (Springer-Verlag, New York, 1985); A. A. Oliner, *Acoustic Surface Waves,* in *Topics in Applied Physics,* Vol. 24 (Springer-Verlag, New York, 1978); *Recent Developments in Surface Acoustic Waves,* edited by D. F. Parker and G. A. Maugin, Springer Series on Wave Phenomena (Springer Verlag, New York, 1988).

[32]J. R. Chamuel and G. H. Brooke, J. Acoust. Soc. Am. **84**, 1363 (1988).

[33]M. Kohmoto, L. P. Kadanoff, and C. Tang, Phys. Rev. Lett. **50**, 1870 (1983).

[34]S. Ostlund, R. Pandit, D. Rand, H. J. Schellnhuber, and E. D. Siggia, Phys. Rev. Lett. **50**, 1873 (1983).

[35]J. M. Luck and D. Petritis, J. Stat. Phys. **42**, 289 (1986).

[36]M. Kohmoto, B. Sutherland, and C. Tang, Phys. Rev. **35**, 1020 (1987).

[37]S. Abe and H. Hiramoto, Phys. Rev. A **36**, 5349 (1987).

[38]M. Kohmoto (unpublished).

[39]C. Tang and M. Kohmoto (unpublished).

[40]M. Kohmoto (unpublished).

[41]D. J. Thouless and Q. Niu, J. Phys. A **16**, 1911 (1983).

[42]A. D. Zdetsis, C. M. Soukoulis, and E. N. Economou, Phys. Rev. B **33**, 4936 (1986).

[43]G. Gumbs and M. K. Ali, Phys. Rev. Lett. **60**, 1081 (1988).

[44]H. Xu, J. Phys. C **20**, 5999 (1987).

[45]A. P. Siebesma and L. Pietronero, Eur. Phys. Lett. **4**, 597 (1987).

[46]T. Janssen and M. Kohmoto (unpublished).

[47]M. Kohmoto, B. Sutherland, and K. Iguchi, Phys. Rev. Lett. **58**, 2436 (1987).

[48]G. Gumbs and M. K. Ali, J. Phys. A **21**, L517 (1988).

[49]S. Das Sarma, A. Kobayashi, and R. E. Prange, Phys. Rev. Lett. **56**, 1280 (1986).

[50]C. Schwartz, Appl. Opt. **27**, 1232 (1988).

[51]J. M. Luck, Phys. Rev. B **39**, 5834 (1989).

[52]H. Hiramoto and M. Kohmoto, Phys. Rev. Lett. **62**, 2714 (1989).

[53]J. P. Lu and J. L. Birman, Phys. Rev. B **38**, 8067 (1988).

[54]R. Merlin, K. Bajema, R. Clarke, F. Y. Juang, and P. K. Bhattacharya, Phys. Rev. Lett. **55**, 1768 (1985).

[55]R. Riklund and M. Severin, J. Phys. C **21**, 3217 (1988).

[56]F. Laruelle and B. Etienne, Phys. Rev. B **37**, 4816 (1988).

[57]P. Hawrylak, G. Eliasson, and J. J. Quinn, Phys. Rev. B **36**, 6505 (1987).

[58]S. He and J. D. Maynard, Phys. Rev. Lett. **62**, 1888 (1989).

[59]J. P. Lu and J. L. Birman, J. Acoust. Soc. Am. Suppl. 1, **87**, TT5 (1990); **87**, S113 (1990).

[60]T.-B. Yuang and A. L. Pate, J. Acoust. Soc. Am. Suppl. 1, **87**, TT5 (1990); **87**, S113 (1990).

[61]M. J. McKenna, P. S. Spoor, R. L. Stanley, E. Dimasi, and J. D. Maynard, J. Acoust. Soc. Am. Suppl. 1, **87**, TT8 (1990); **87**,

S113 (1990).
[62]D. T. Smith, C. P. Lorenson, R. B. Hallock, K. R. McCall, and R. A. Guyer, Phys. Rev. Lett. **40**, 6634 (1989).
[63]L. Landau and E. Lifschitz, *Théorie de L'élasticité* (MIR, Moscow, 1967).
[64]L. J. Bond, Ultrasonics, 71 (1979).
[65]H. S. Tuan and J. P. Parekh, IEEE Trans. Sonics Ultrason. **SU24**, 384 (1977).
[66]S. D. Wu and H. S. Tuan, J. Appl. Phys. **50**, 73 (1979).
[67]O. W. Otto, IEEE Trans. Sonics Ultrason. **SU22**, 251 (1975).
[68]N. E. Glass and A. A. Maradudin, J. Appl. Phys. **54**, 796 (1983); E. L. Cambiaggio and F. C. Cuozzo, IEEE Trans. Sonics Ultrason. **SU26**, 340 (1979); A. Ronnekleiv and J. Souquet, Ultrasonics Symp. Proc. IEEE **75**, CHO 994-4SU, 1975; J. Appl. Phys. **47**, 4422 (1976); J. Menngailis, R. C. Williamson, J. Holtham, and R. C. M. Li, Wave Electron. **2**, 177 (1976).
[69]E. Baron, Thèse de Troisième Cycle, Paris 7 (1986); E. Baron, M. de Billy, and G. Quentin, Rev. Phys. Appl. **20**, 369 (1985).
[70]D. Sornette, L. Macon, and J. Coste, J. Phys. (Paris) **49**, 1683 (1988).
[71]D. Levine and P. J. Steinhardt, Phys. Rev. B **34**, 596 (1986); Phys. Rev. Lett. **53**, 2477 (1984).
[72]W. Narkiewicz and S. Kanemitsu, *Number Theory* (World Scientific, Singapore, 1983), Chap. 8.
[73]R. K. P. Zia and W. J. Dallas, J. Phys. A **18**, L341 (1985).
[74]The quantitative analysis of the spectrum and in particular the determination of the diophantine approximation of at/λ are very sensitive to the precision with which the mode frequency and the SAW velocity is measured. In fact, the frequency is determined with a precision better than 10^{-4} so that the limiting factor is the determination of the wave velocity c_R. In the impulse response we have a mean to determine c_R (see Sec. III E), but this corresponds to a group velocity which is slightly different from the phase velocity at a particular frequency. Indeed, if a planar surface is not dispersive, which gaurantees the equality between group and phase velocity, this is no more true in the presence of a quasiperiodic corrugation. This explains the (small) difference between the group velocity $\approx 3473 \pm 6$ ms^{-1} measured in Sec. III E and the phase velocity ≈ 3495 m/s at frequencies around $f = 166$ MHz. This value has been chosen such that the representation of at/λ as a sum of reciprocal lattice vectors correctly describes the observed structure of the proper modes. In other words, if one believes in the critical mode theory (Ref. 36) the analysis of the spatial structure of the modes and of their different wavelengths gives a mean to determine the phase SAW velocity in presence of the quasiperiodic modulation.
[75]L. Macon, D. Sornette, and J. Coste, in *Electromagnetic and Acoustic Scattering: Detection and Inverse Problem,* edited by C. Bourrely, P. Chiapetta, and B. Torrensani (World Scientific, Singapore, 1989), p. 165.